Electronic Supplementary Material (ESI) for Physical Chemistry Chemical Physics.

Supporting Information

Divalent *closo*-monocarborane solvates for solid-state ionic conductors.

Authors: *Amanda Berger[1], Ainee Ibrahim[1], Craig E. Buckley[1], and Mark Paskevicius[1]*

[1]Department of Physics and Astronomy, Fuels and Energy Technology Institute, Curtin University, GPO Box U1987, Perth, WA 6845, Australia.

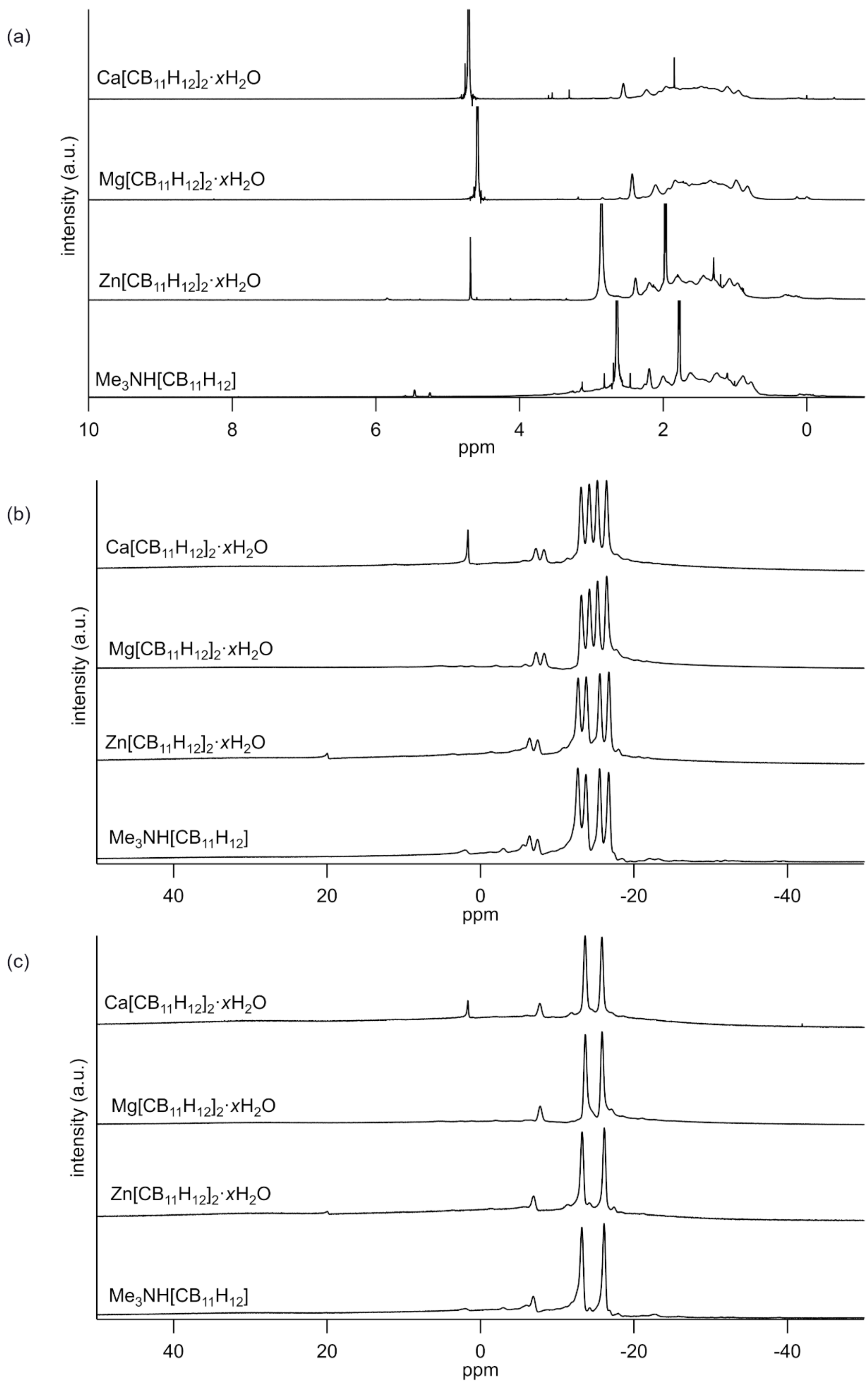

Figure S1:(a) ^{1}H, (b) ^{11}B and (c) $^{11}B\{^{1}H\}$ NMR of $Me_3NH[CB_{11}H_{12}]$ and hydrated divalent salts $Zn[CB_{11}H_{12}]_2{\cdot}xH_2O$, $Mg[CB_{11}H_{12}]_2{\cdot}xH_2O$, and $Ca[CB_{11}H_{12}]_2{\cdot}xH_2O$. $Me_3NH[CB_{11}H_{12}]$ and

$Zn[CB_{11}H_{12}]_2 \cdot xH_2O$ samples were analysed in CD_3CN. $Mg[CB_{11}H_{12}]_2 \cdot xH_2O$, and $Ca[CB_{11}H_{12}]_2 \cdot xH_2O$ were analysed in D_2O. Solvents differ due to solubility issues..

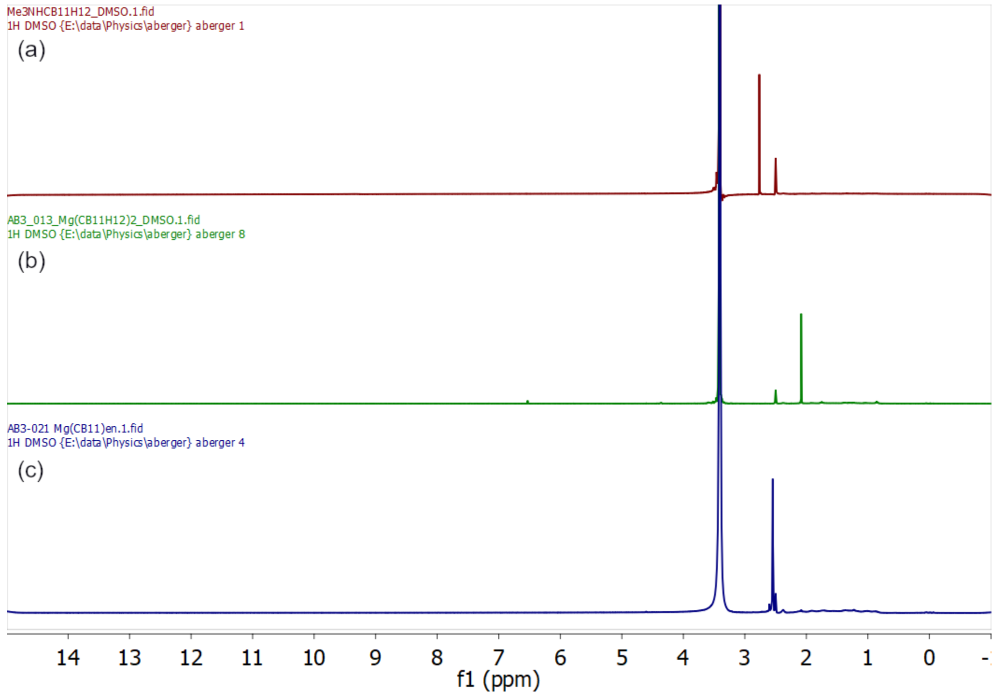

Figure S2: ^{1}H NMR of (a) $Me_3NH[CB_{11}H_{12}]$, (b) $Mg[CB_{11}H_{12}]_2$ and (c) $Mg[CB_{11}H_{12}]_2 \cdot 3en$ in DMSO-*d6.*

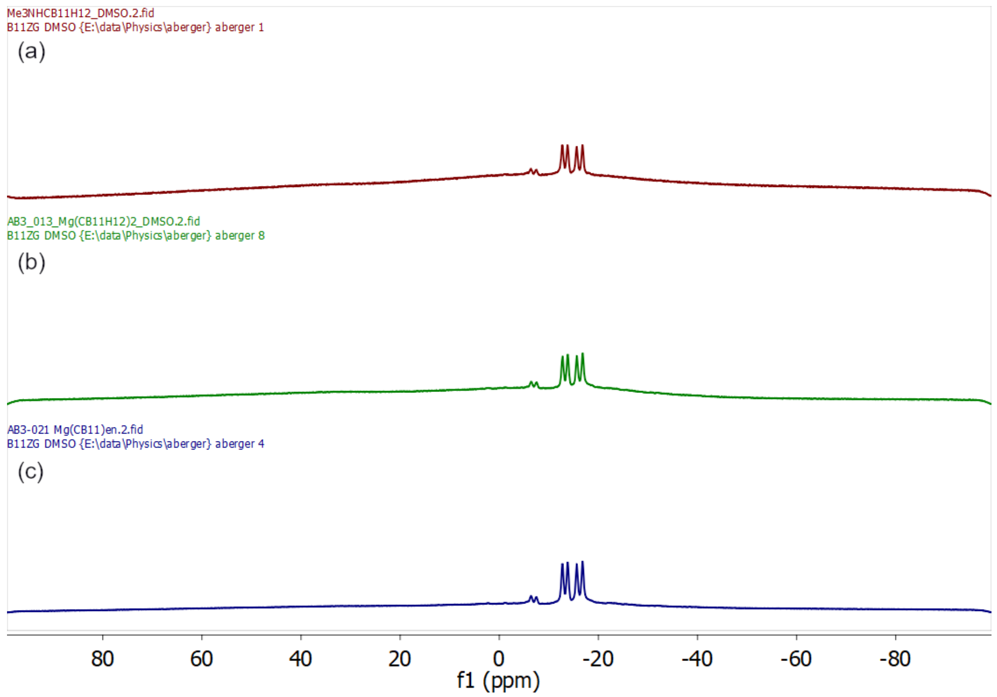

Figure S3: ^{11}B NMR of (a) $Me_3NH[CB_{11}H_{12}]$, (b) $Mg[CB_{11}H_{12}]_2$ and (c) $Mg[CB_{11}H_{12}]_2 \cdot 3en$ in DMSO-*d6.*

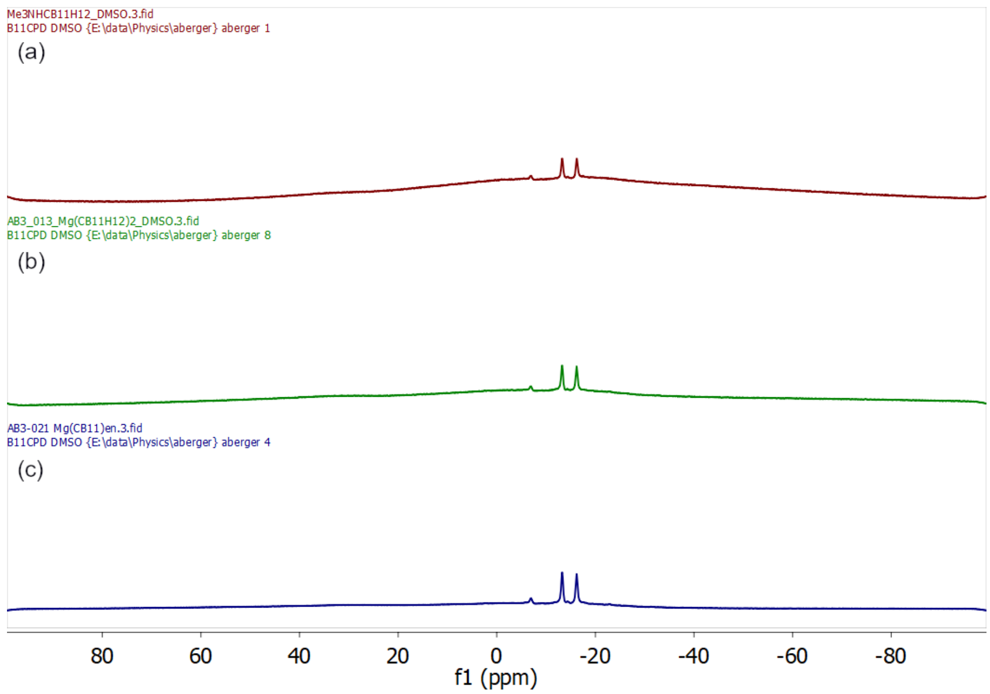

Figure S4: $^{11}B\{^{1}H\}$ NMR of (a) $Me_3NH[CB_{11}H_{12}]$, (b) $Mg[CB_{11}H_{12}]_2$ and (c) $Mg[CB_{11}H_{12}]_2{\cdot}3en$ in DMSO-*d6.*

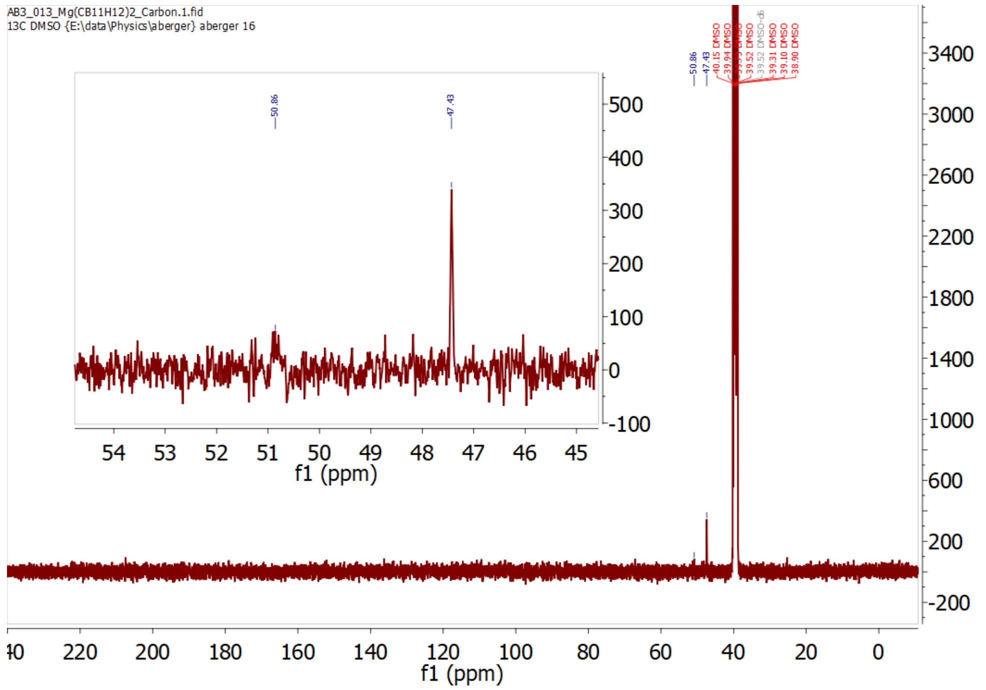

Figure S5: $^{13}C\{^{1}H\}$ NMR of $Mg[CB_{11}H_{12}]_2$ in DMSO-*d6.*

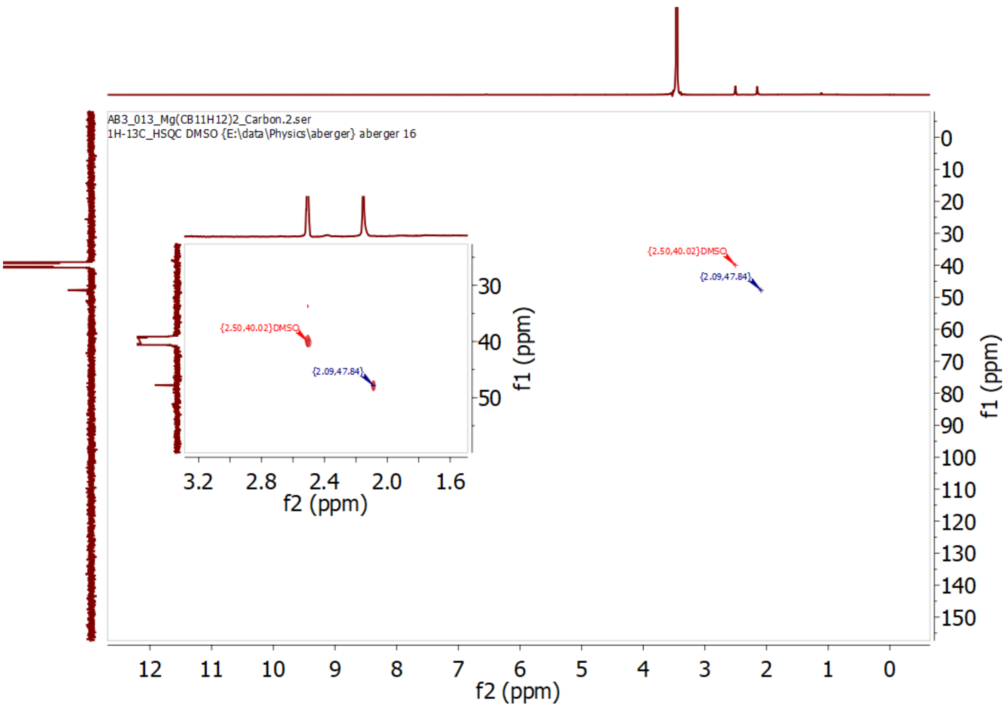

Figure S6: ^{1}H-^{13}C HSQC of $Mg[CB_{11}H_{12}]_2$ in DMSO-*d6*.

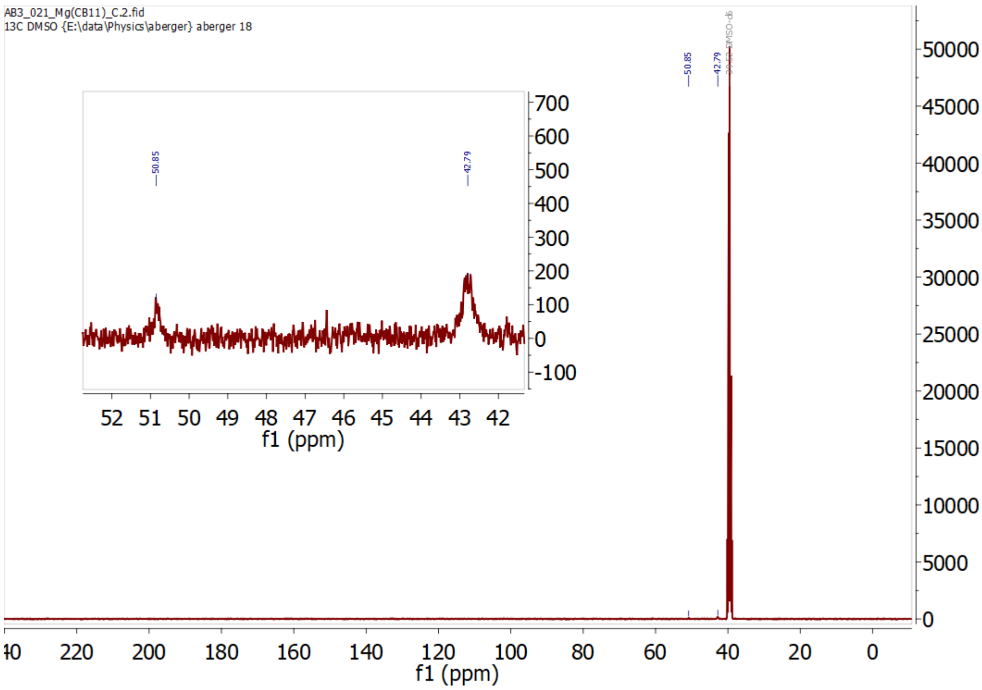

Figure S7: $^{13}C\{^{1}H\}$ NMR of $Mg[CB_{11}H_{12}]_2\cdot 3en$ in DMSO-*d6.*

Table S1: Estimation of residual water for $Mg[CB_{11}H_{12}]_2{\cdot}xH_2O$, $Ca[CB_{11}H_{12}]_2{\cdot}xH_2O$ and $Zn[CB_{11}H_{12}]_2{\cdot}xH_2O$ dried at different temperatures. Estimation was calculated from thermogravimetric analysis (TGA) residual masses.

Sample	Temp dried (°C)	Initial mass (mg)	Residual (%)	Ratio mol $M[CB_{11}H_{12}]_2$	Ratio mol H_2O	In text notation
$Mg[CB_{11}H_{12}]_2{\cdot}xH_2O$	100	5.00	84.7%	1	3.1	$Mg[CB_{11}H_{12}]_2{\cdot}3.1H_2O$
$Ca[CB_{11}H_{12}]_2{\cdot}xH_2O$	100	3.55	90.7%	1	1.9	$Ca[CB_{11}H_{12}]_2{\cdot}1.9H_2O$
$Ca[CB_{11}H_{12}]_2{\cdot}xH_2O$	125	4.57	95.7%	1	0.8	$Ca[CB_{11}H_{12}]_2{\cdot}0.8H_2O$
$Zn[CB_{11}H_{12}]_2.{\cdot}xH_2O$	100	4.67	86.5%	1	3.0	$Zn[CB_{11}H_{12}]_2{\cdot}3H_2O$
$Zn[CB_{11}H_{12}]_2{\cdot}xH_2O$	150	4.18	90.9%	1	1.9	$Zn[CB_{11}H_{12}]_2{\cdot}1.9H_2O$
$Ca[B_{12}H_{12}]{\cdot}xH2O$	100	3.08	85.7%	1	1.7	$Ca[B_{12}H_{12}]{\cdot}1.7H2O$
$Zn[B_{12}H_{12}]{\cdot}xH2O$	100	1.85	80.8%	1	2.7	$Zn[B_{12}H_{12}]{\cdot}2.7H2O$

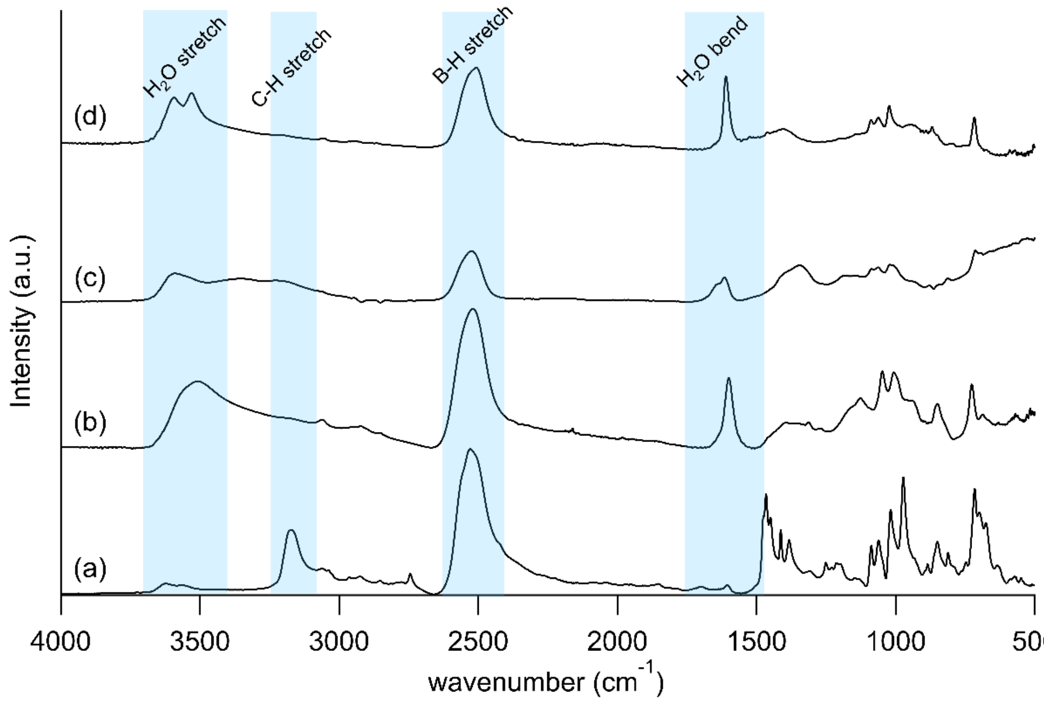

Figure S8: FTIR of (a) $Me_3NH[CB_{11}H_{12}]$, (b) $Zn[CB_{11}H_{12}]_2{\cdot}xH_2O$, (c) $Mg[CB_{11}H_{12}]_2{\cdot}xH_2O$ and (d) $Ca[CB_{11}H_{12}]_2{\cdot}xH_2O$. All samples were dried at 100 °C before analysis.

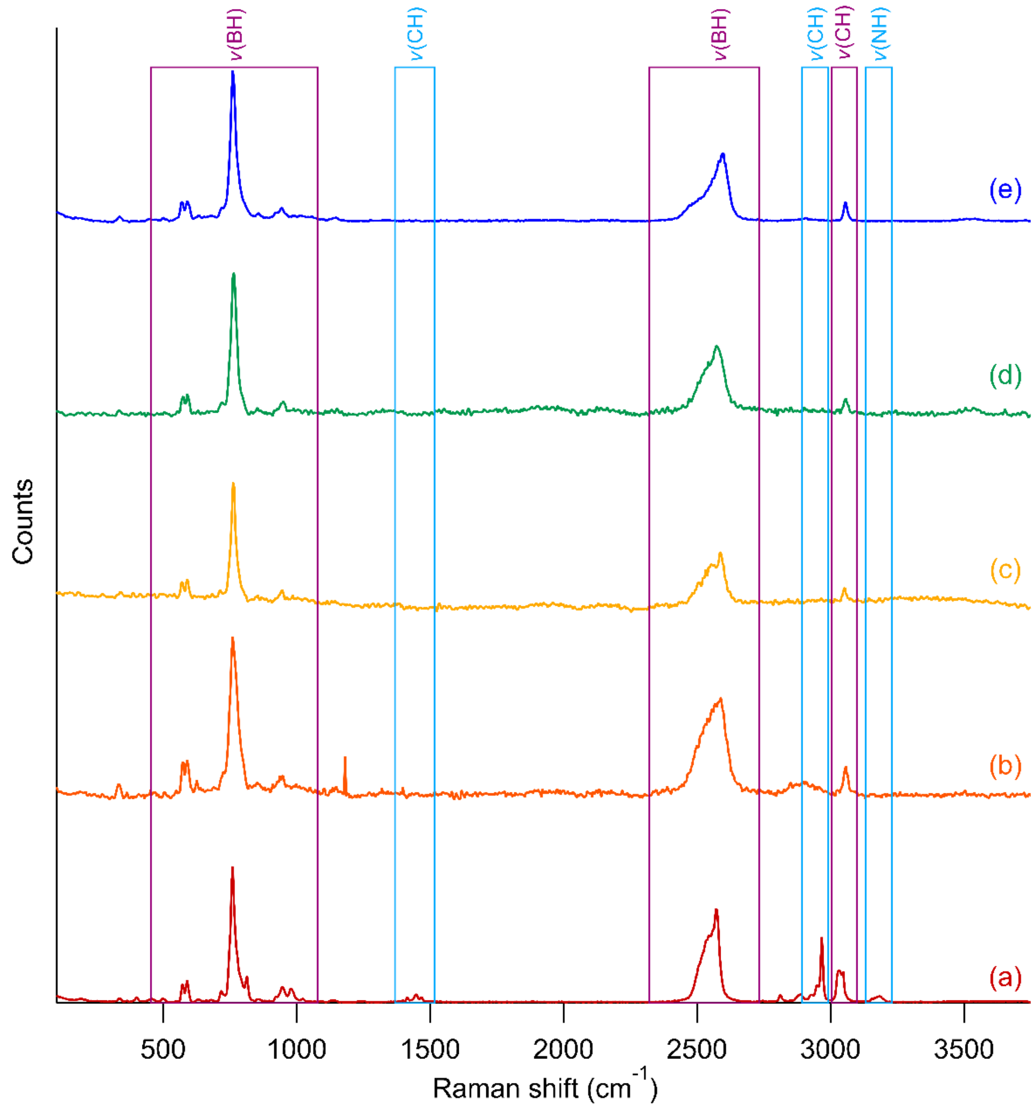

Figure S9: Raman spectra for (a) $Me_3NH[CB_{11}H_{12}]$, (b) $Na[CB_{11}H_{12}]$, (c) $Zn[CB_{11}H_{12}]_2.xH_2O$, (d) $Mg[CB_{11}H_{12}]_2.xH_2O$ and (e) $Ca[CB_{11}H_{12}]_2.xH_2O$. Purple boxes indicate features attributed to the anion $[CB_{11}H_{12}]^-$, whereas blue boxes are due to the cation Me_3NH^+. All samples were dried at 100 °C before analysis.

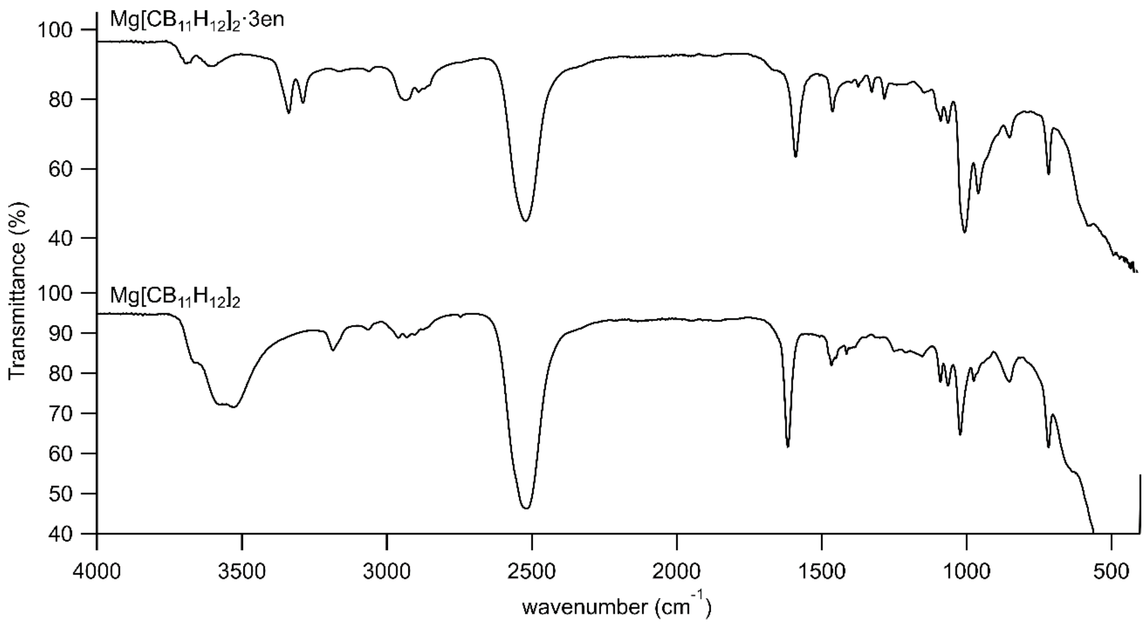

Figure S10: FTIR of $Mg[CB_{11}H_{12}]_2$ and $Mg[CB_{11}H_{12}]_2·3en$. All samples were briefly exposed to air during measurement. All samples were dried at 100 °C for 1 hour before analysis.

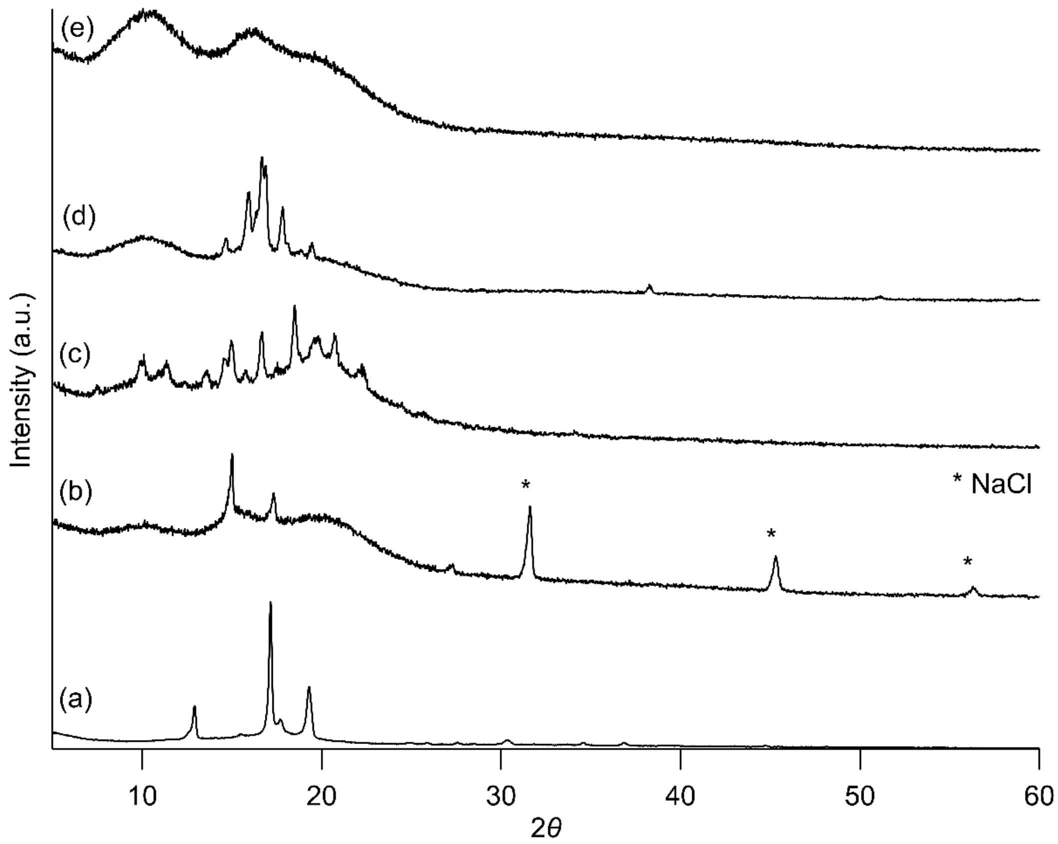

Figure S11: pXRD of (a) $Me_3NH[CB_{11}H_{12}]$, (b) $Na[CB_{11}H_{12}]$, (c) $Zn[CB_{11}H_{12}]_2{\cdot}xH_2O$, (d) $Mg[CB_{11}H_{12}]_2{\cdot}xH_2O$, and (e) $Ca[CB_{11}H_{12}]_2{\cdot}xH_2O$. $Me_3NH[CB_{11}H_{12}]$ was prepared in air using a standard pXRD holder, whereas $Na[CB_{11}H_{12}]$, $Zn[CB_{11}H_{12}]_2{\cdot}xH_2O$, $Mg[CB_{11}H_{12}]_2{\cdot}xH_2O$ and $Ca[CB_{11}H_{12}]_2{\cdot}xH_2O$ were prepared in an Ar filled glovebox using air-tight dome holders to prevent the absorption of atmospheric moisture. All samples were dried at 100 °C before analysis. CuKα radiation source (λ = 1.5406 Å) Data was collected from 5 – 60° 2ϑ at 0.02° steps over 1 hour.

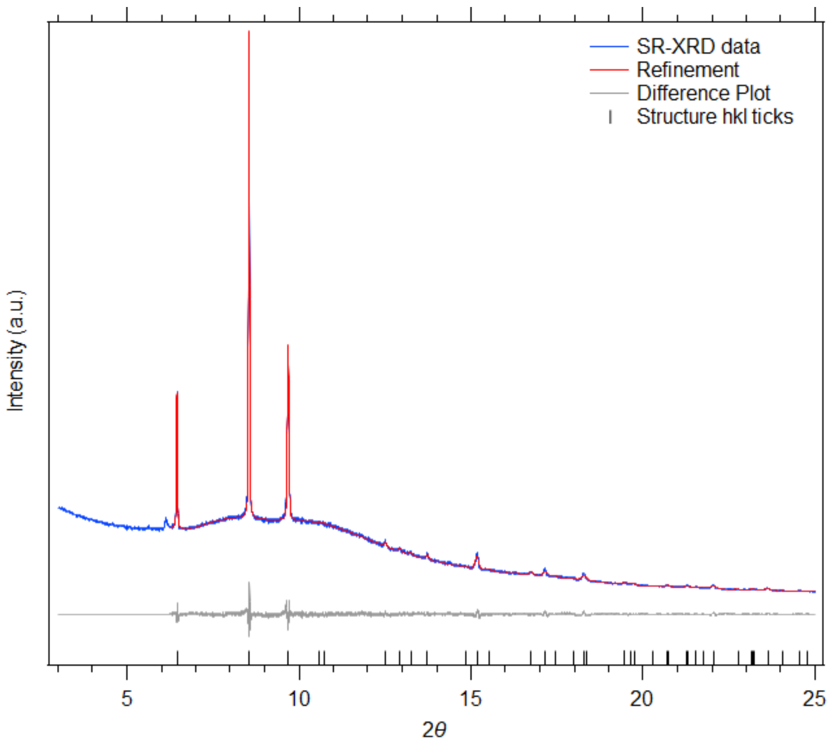

Figure S12: SR-XRD of $Mg[CB_{11}H_{12}]_2$ compared to the Topas refinement of the data. The energy of the X-ray beam was 16 keV (λ = 0.774954(1) Å)

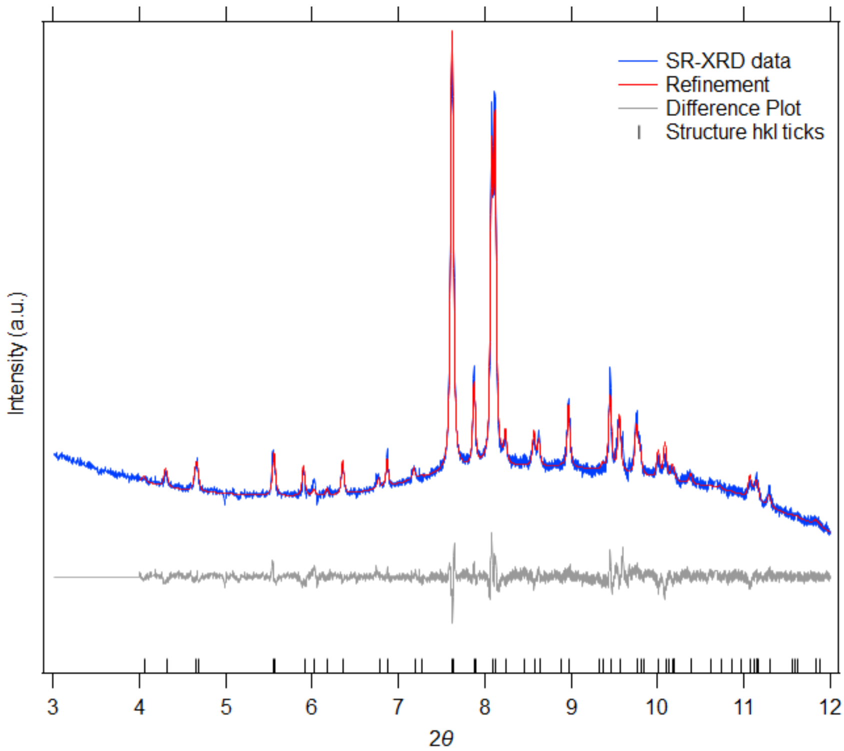

Figure S13: SR-XRD of $Mg[CB_{11}H_{12}]_2{\cdot}3en$ compared to the Topas refinement of the data. The energy of the X-ray beam was 16 keV (λ = 0.774954(1) Å)

Table S2: Structural parameters for $Mg[CB_{11}H_{12}]_2 \cdot 3en$ at 25.1 °C in space group *Pbca* from Topas refinement of SR-XRD data.

Name	Atom	Wyckoff	*x/a*	*y/b*	*z/c*
Mg1	Mg	8	0.72580	0.64451	0.59790
N1	N	8	0.60280	0.69880	0.57960
H1	H	8	0.58500	0.70630	0.52790
H2	H	8	0.61000	0.74120	0.60210
N2	N	8	0.62400	0.57290	0.62210
H3	H	8	0.62000	0.56590	0.67550
H4	H	8	0.63800	0.53150	0.59900
C1	C	8	0.52820	0.66500	0.61410
H5	H	8	0.53520	0.67100	0.67120
H6	H	8	0.46110	0.68300	0.59900
C2	C	8	0.53530	0.59700	0.59710
H7	H	8	0.47720	0.57200	0.61960
H8	H	8	0.53250	0.59000	0.53980
N3	N	8	0.84750	0.58860	0.62820
H9	H	8	0.89350	0.58380	0.58780
H10	H	8	0.83100	0.54540	0.64480
N4	N	8	0.75060	0.68130	0.69930
H11	H	8	0.76600	0.72720	0.69580
H12	H	8	0.69350	0.67870	0.73030
C3	C	8	0.89370	0.62320	0.68510
H13	H	8	0.93020	0.66100	0.65950
H14	H	8	0.94500	0.59600	0.71290
C4	C	8	0.82370	0.64770	0.73660
H15	H	8	0.79100	0.60960	0.76440
H16	H	8	0.85730	0.67600	0.77690
N5	N	8	0.81400	0.71070	0.53850
H17	H	8	0.79900	0.75450	0.55460
H18	H	8	0.88200	0.70390	0.54930
N6	N	8	0.72360	0.60590	0.48260
H19	H	8	0.72880	0.55900	0.47910
H20	H	8	0.66330	0.61740	0.45840
C5	C	8	0.80000	0.70370	0.46190
H21	H	8	0.85300	0.72600	0.43090
H22	H	8	0.73500	0.72470	0.44810
C6	C	8	0.79780	0.63590	0.44300
H23	H	8	0.86270	0.61500	0.45810
H24	H	8	0.79000	0.63100	0.38570
B1a	B	8	0.49000	0.79700	0.75600
B2a	B	8	0.50000	0.86000	0.69900
B3a	B	8	0.57000	0.92000	0.74000
B4a	B	8	0.61000	0.89000	0.82300
B5a	B	8	0.44000	0.82000	0.83400
B6a	B	8	0.56000	0.81000	0.83300

B7a	B	8	0.40000	0.85000	0.75000
B8a	B	8	0.45000	0.92000	0.74000
B9a	B	8	0.52000	0.94100	0.81700
B10a	B	8	0.51000	0.87700	0.87400
B11a	B	8	0.41000	0.90000	0.82300
H1a	H	8	0.65000	0.82000	0.73000
H2a	H	8	0.50000	0.75000	0.73000
H3a	H	8	0.51000	0.85000	0.63700
H4a	H	8	0.63000	0.94000	0.71000
H5a	H	8	0.68000	0.89000	0.84000
H6a	H	8	0.39000	0.79000	0.87000
H7a	H	8	0.60000	0.77000	0.86000
H8a	H	8	0.33000	0.84000	0.72000
H9a	H	8	0.42000	0.96000	0.71000
H10a	H	8	0.50000	0.99000	0.84000
H11a	H	8	0.51000	0.88000	0.93600
H12a	H	8	0.35000	0.92000	0.85000
C1a	C	8	0.59000	0.84000	0.75300
B1b	B	8	0.18000	0.96400	0.11500
B2b	B	8	0.14000	0.97500	0.03000
B3b	B	8	0.07500	0.91000	0.00400
B4b	B	8	0.08000	0.85700	0.08000
B5b	B	8	0.25600	0.90000	0.11300
B6b	B	8	0.14000	0.89000	0.14400
B7b	B	8	0.25000	0.95000	0.04000
B8b	B	8	0.19000	0.92000	-0.02700
B9b	B	8	0.15000	0.84600	0.00200
B10b	B	8	0.19000	0.83500	0.09000
B11b	B	8	0.26000	0.87000	0.03000
H1b	H	8	0.02000	0.95000	0.11000
H2b	H	8	0.18000	1.01000	0.15000
H3b	H	8	0.11000	1.02400	0.01000
H4b	H	8	0.01000	0.91000	-0.03000
H5b	H	8	0.01000	0.83000	0.09000
H6b	H	8	0.32000	0.90000	0.15000
H7b	H	8	0.12000	0.88000	0.20300
H8b	H	8	0.31000	0.99000	0.03000
H9b	H	8	0.20000	0.93000	-0.08700
H10b	H	8	0.14000	0.80000	-0.04000
H11b	H	8	0.21000	0.78500	0.11000
H12b	H	8	0.33000	0.85000	0.00000
C1b	C	8	0.07800	0.93000	0.09000

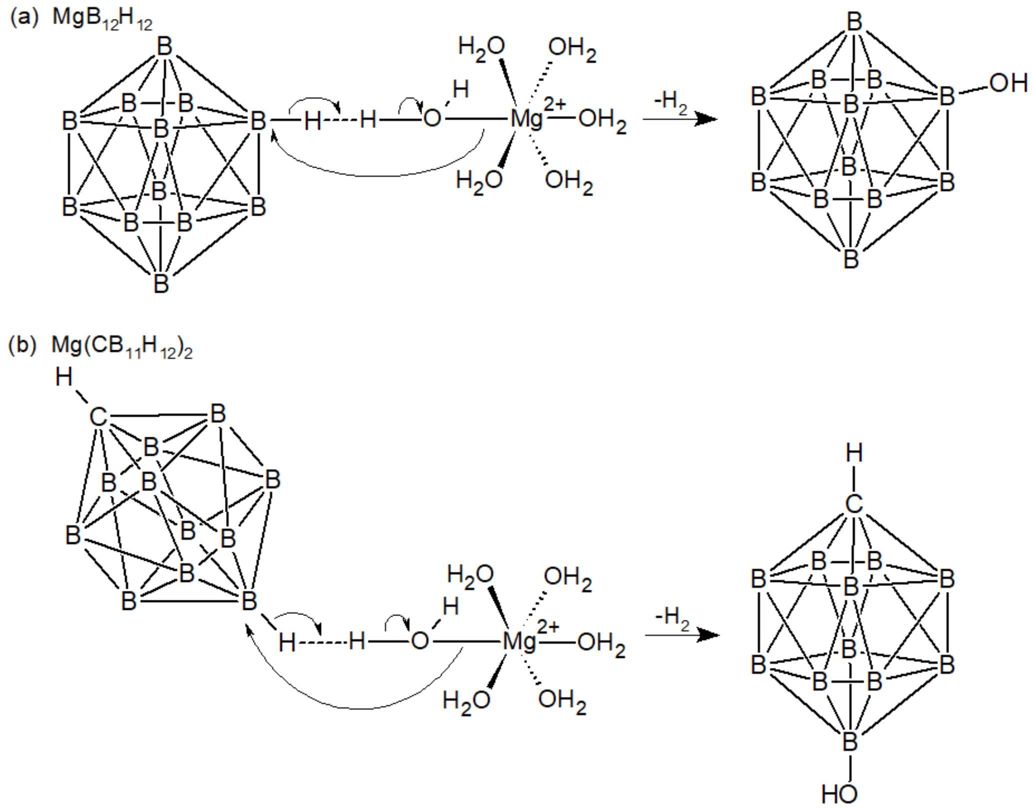

Scheme S1: Mechanism for the hydroxylation of (a) $Mg(H_2O)_3[B_{12}H_{12}]$ proposed by Shore et al.[1], and (b), is proposed for $Mg[CB_{11}H_{12}]_2{\cdot}xH_2O$.

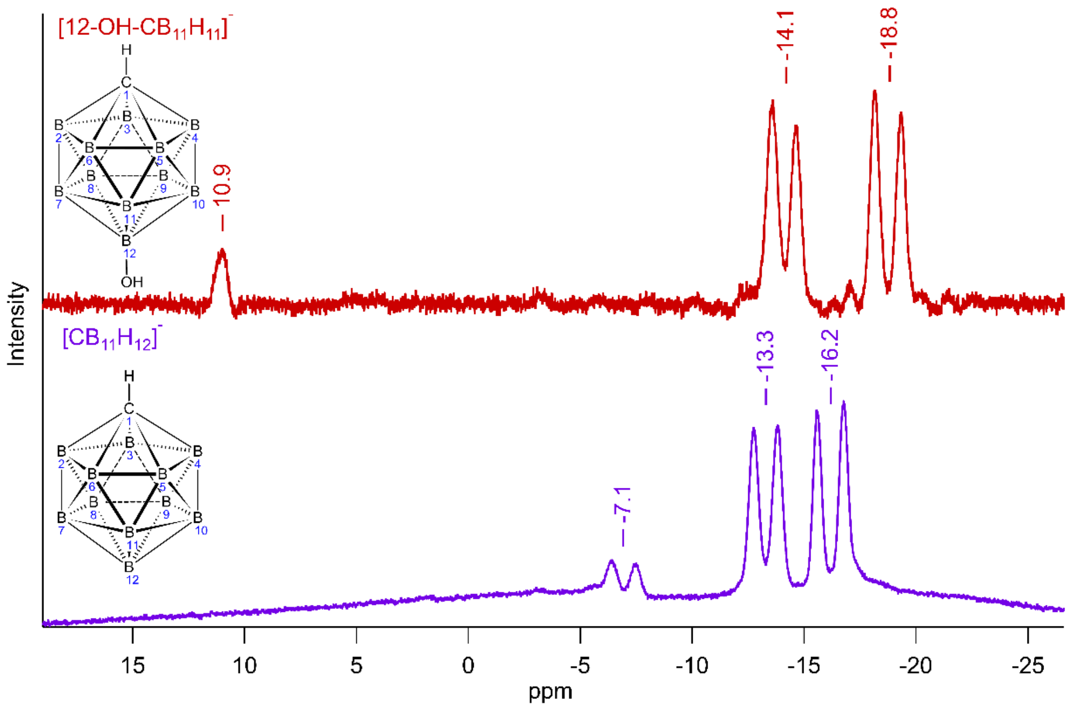

Figure S14: [11]B NMR (CD_3CN) of the $[CB_{11}H_{12}]^-$ anion (purple) and $[12\text{-}OH\text{-}CB_{11}H_{11}]^-$ anion (red).

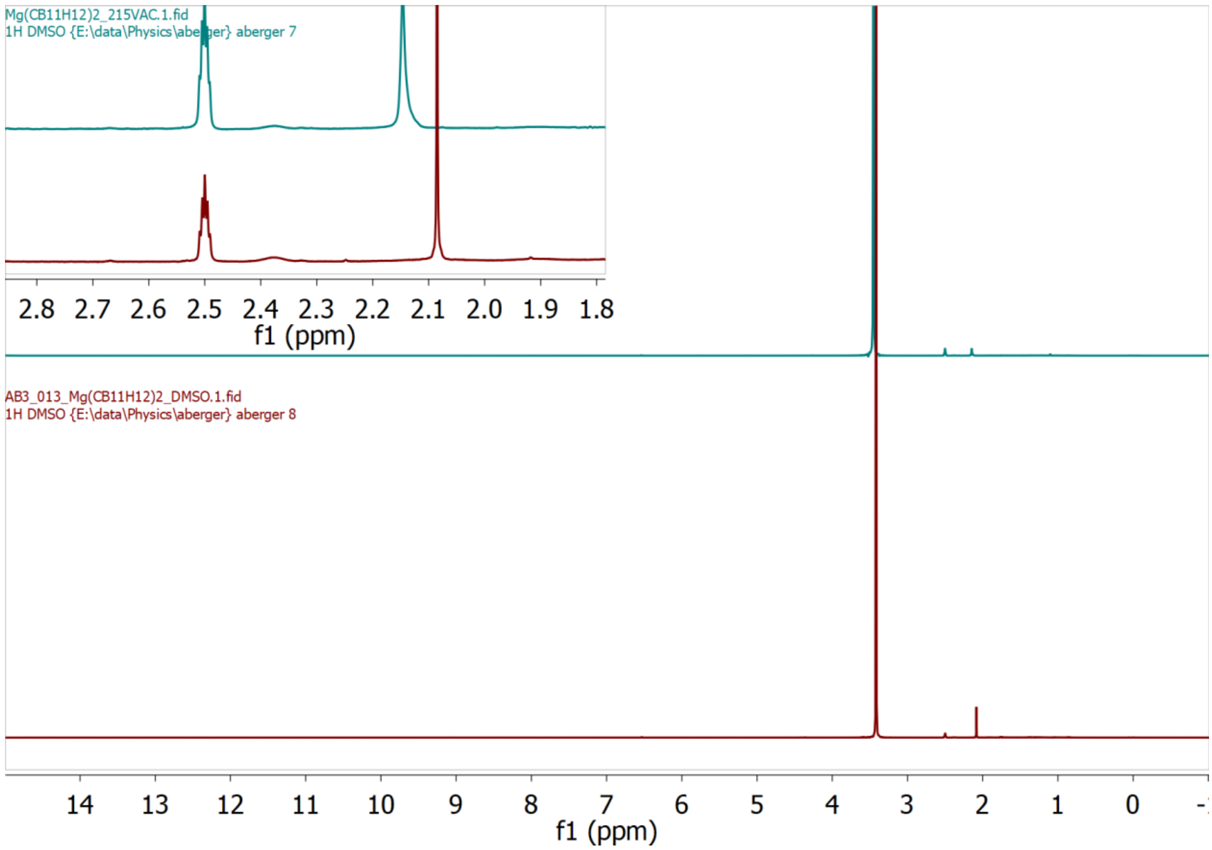

Figure S15: [1]H NMR of $Mg[CB_{11}H_{12}]_2$ dried at 100 °C (bottom) and $Mg[CB_{11}H_{12}]_2$ heated under vacuum to 215 °C (top) in DMSO-*d6*. Inset shows a closer observation of peaks between 2.9 and 1.8 ppm.

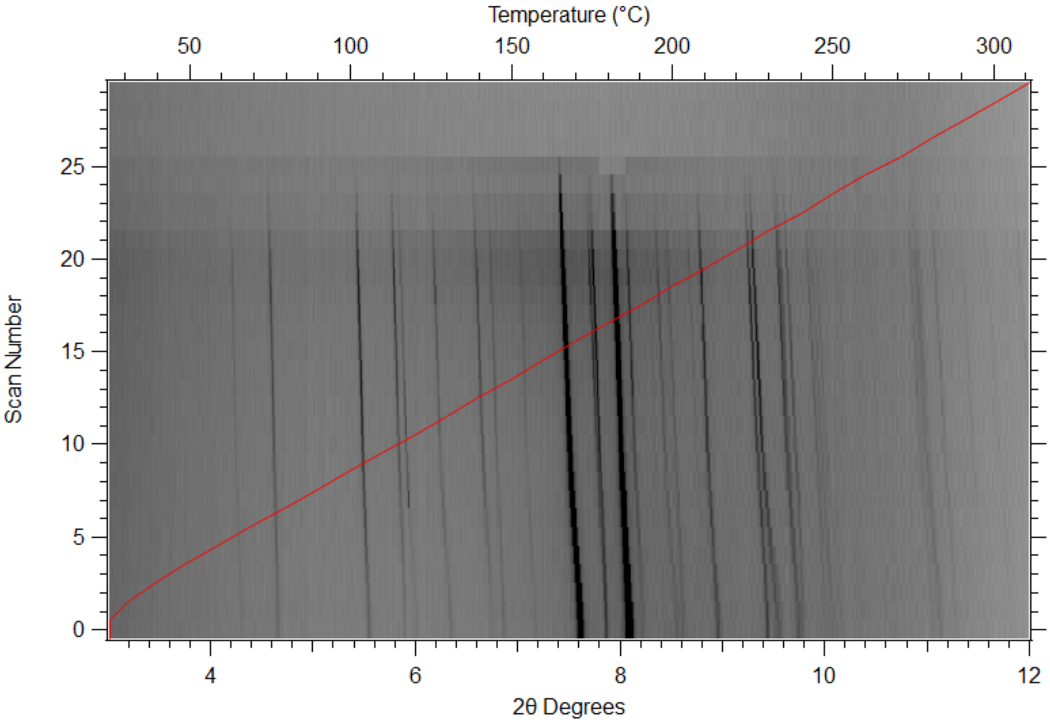

Figure S16: SR-XRD *in situ* ramp of $Mg[CB_{11}H_{12}]_2{\cdot}3en$ from 25 °C to 300 °C.

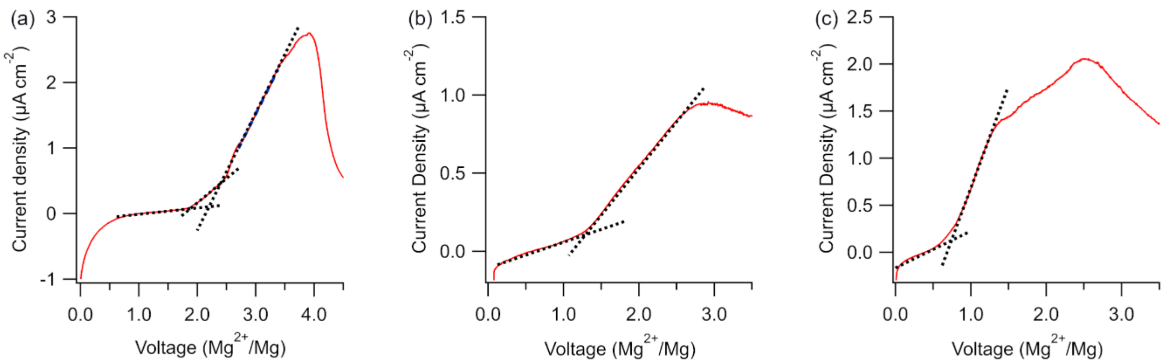

Figure S17: Linear sweep voltammetry (LSV) of (a) $Mg[CB_{11}H_{12}]_2{\cdot}3.1H_2O$, (b) $Mg[CB_{11}H_{12}]_2$, and (c) $Mg[CB_{11}H_{12}]_2{\cdot}3en$. For LSV, cells were prepared as Mg/electrolyte/electrolyte+C/Pt and were analysed at 100 °C at 50 µV/s due to the low conductivity of the salts. Open circuit voltage (OCV) values were 0.96 V for $Mg[CB_{11}H_{12}]_2{\cdot}3.1H_2O$, 1.08 V for $Mg[CB_{11}H_{12}]_2$, and 0.51 V for $Mg[CB_{11}H_{12}]_2{\cdot}3en$.

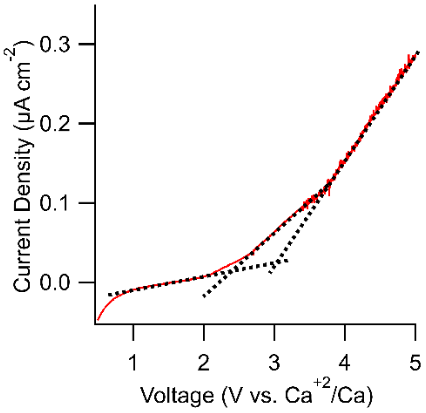

Figure S18: Linear sweep voltammetry (LSV) of $Ca[CB_{11}H_{12}\cdot 1.9H_2O$. For LSV cells were prepared as $Ca/Ca[CB_{11}H_{12}]_2\cdot 1.9H_2O$@100 °C/$Ca[CB_{11}H_{12}]_2\cdot 1.9H_2O$@100 °C+C/Pt with a scan rate of 50 µV s^{-1}. LSV was measured at 100 °C due to the low ionic conductivity at lower temperatures.[18] OCV for $Ca[CB_{11}H_{12}]_2\cdot 1.9H_2O$ was 1.26 V.

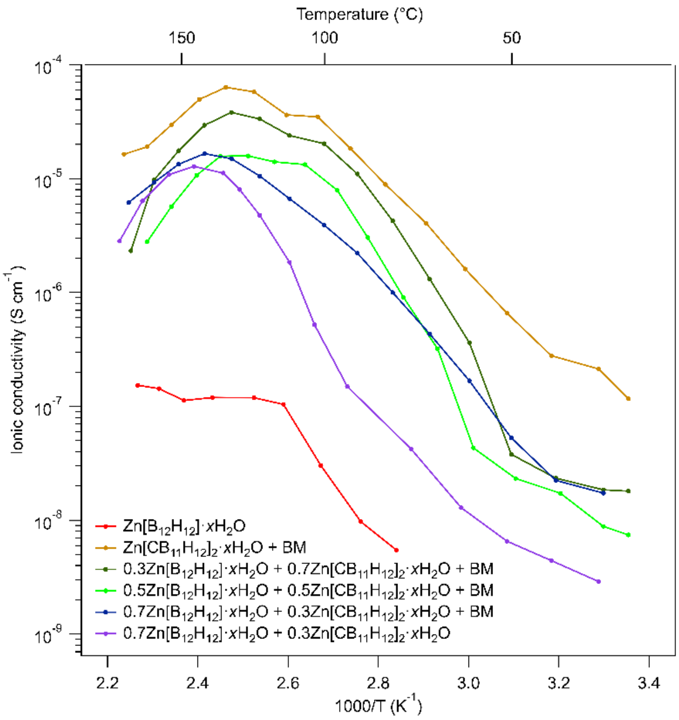

Figure S19: Ionic conductivities of $Zn[CB_{11}H_{12}]_2\cdot xH_2O$, $Zn[B_{12}H_{12}]\cdot xH_2O$ and mixtures with different stoichiometry's. Each sample molar ratio is indicated by the number in front, for example $0.7Zn[B_{12}H_{12}]\cdot xH_2O + 0.3Zn[CB_{11}H_{12}]_2\cdot xH_2O$. The samples labelled + BM were prepared by ball milling the mixtures together for 1 hour in a stainless steel planetary ball mill (Across Industries). Ball sizes were 0.6 mm with a ball to sample mass ratio of 33:1. The sample, $0.7Zn[B_{12}H_{12}]\cdot xH_2O + 0.3Zn[CB_{11}H_{12}]_2\cdot xH_2O$ was prepared by dissolving the appropriate amounts of $Zn[B_{12}H_{12}]\cdot xH_2O$ and $Zn[CB_{11}H_{12}]_2\cdot xH_2O$ in deionised water and drying 16 hours at 100 °C.

NMR data for $Zn[B_{12}H_{12}]$, $Ca[B_{12}H_{12}]$ and $Zn[B_{12}H_{12}]\cdot xH_2O$ + $Zn[CB_{11}H_{12}]_2\cdot xH_2O$ mixed samples.

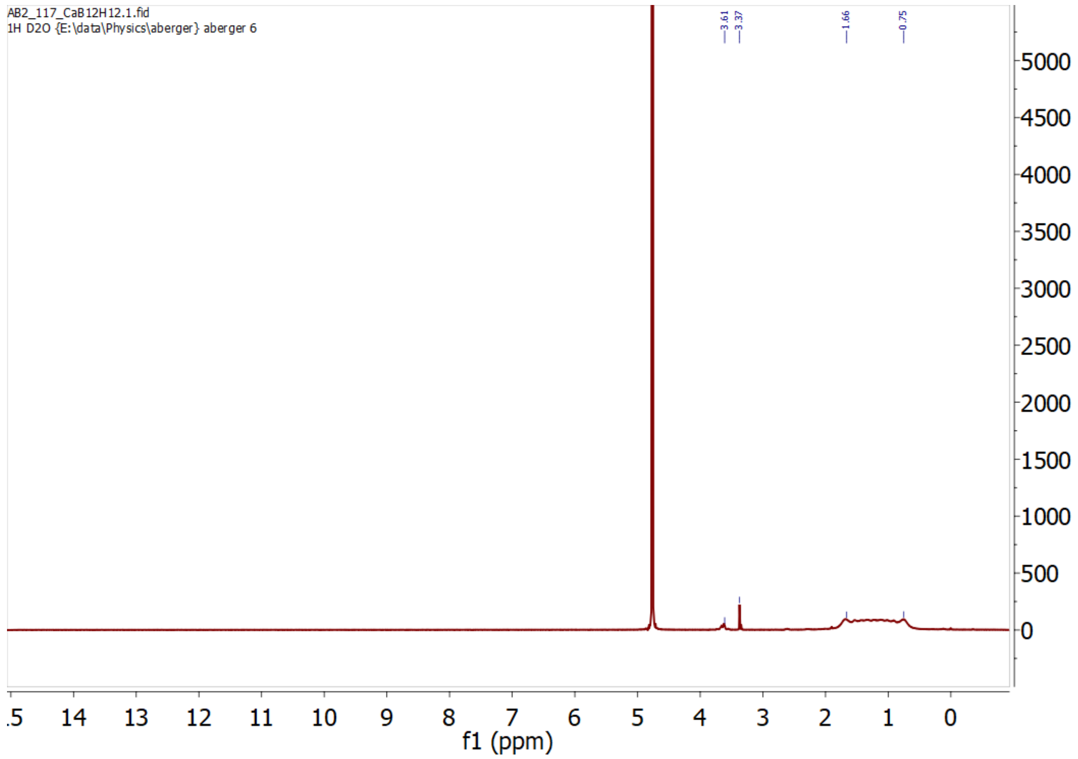

Figure S20: ^{1}H NMR for $Ca[B_{12}H_{12}]\cdot xH_2O$

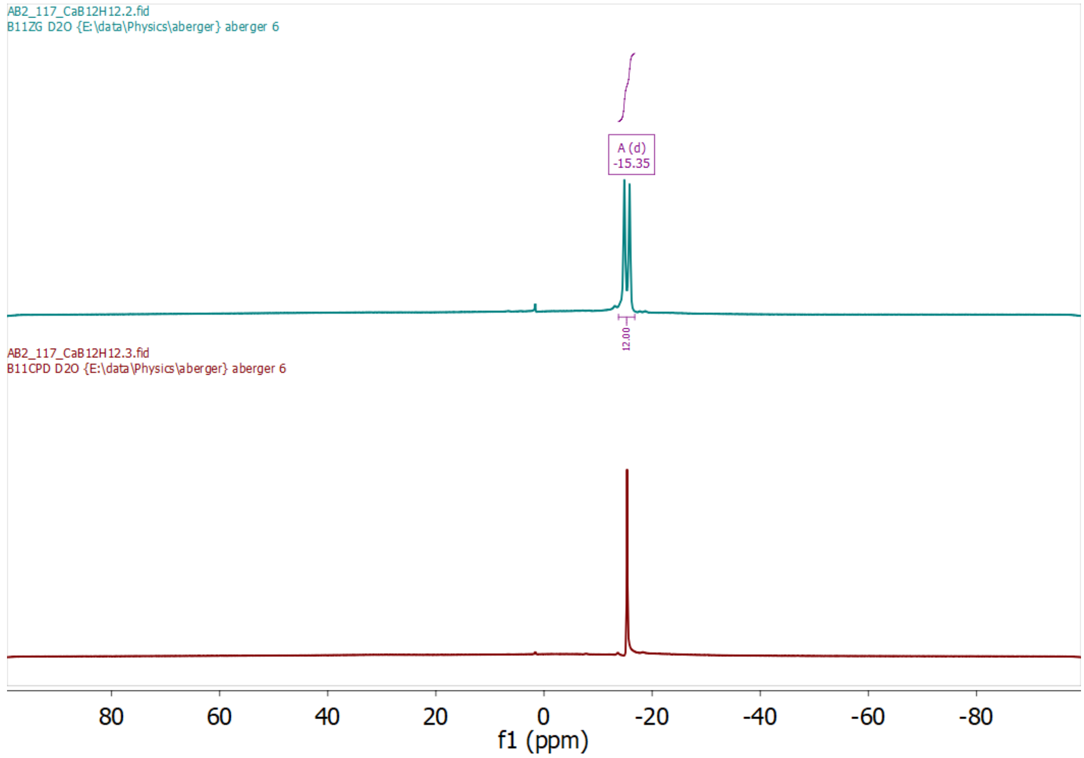

Figure S21: ^{11}B NMR (top) ad $^{11}B\{^{1}H\}$ NMR (bottom) for $Ca[B_{12}H_{12}]\cdot xH_2O$.

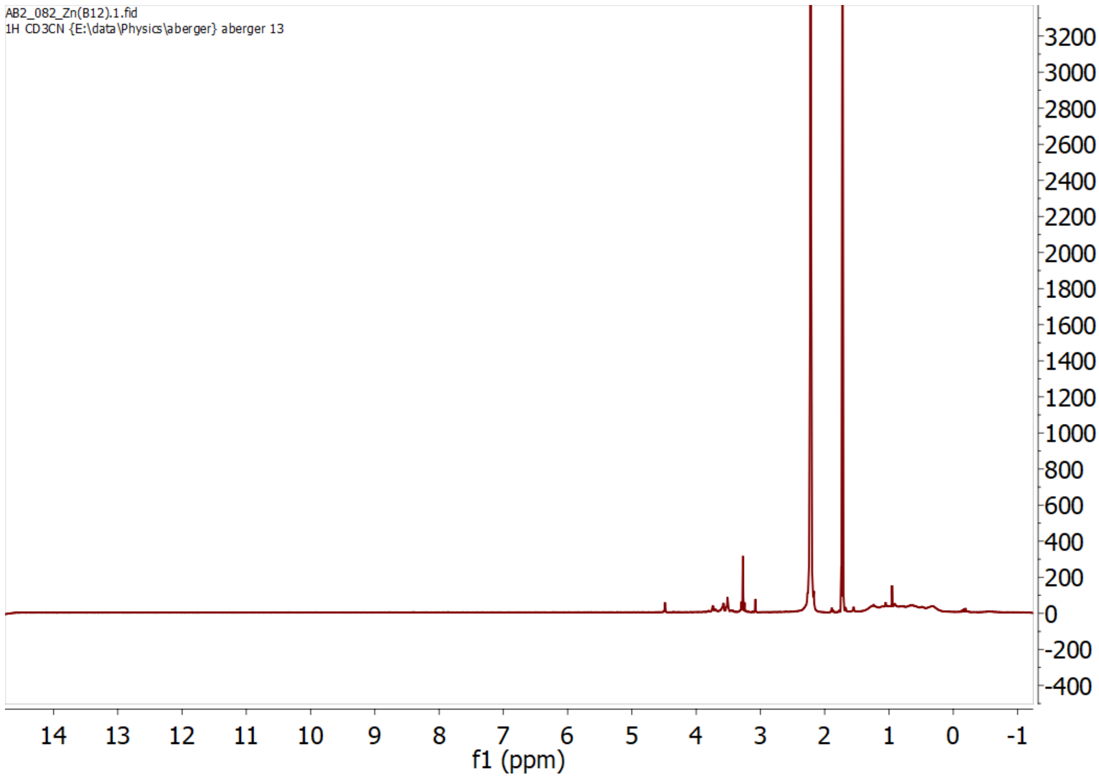

Figure S22: ^{1}H NMR for $Zn[B_{12}H_{12}]\cdot xH_2O$

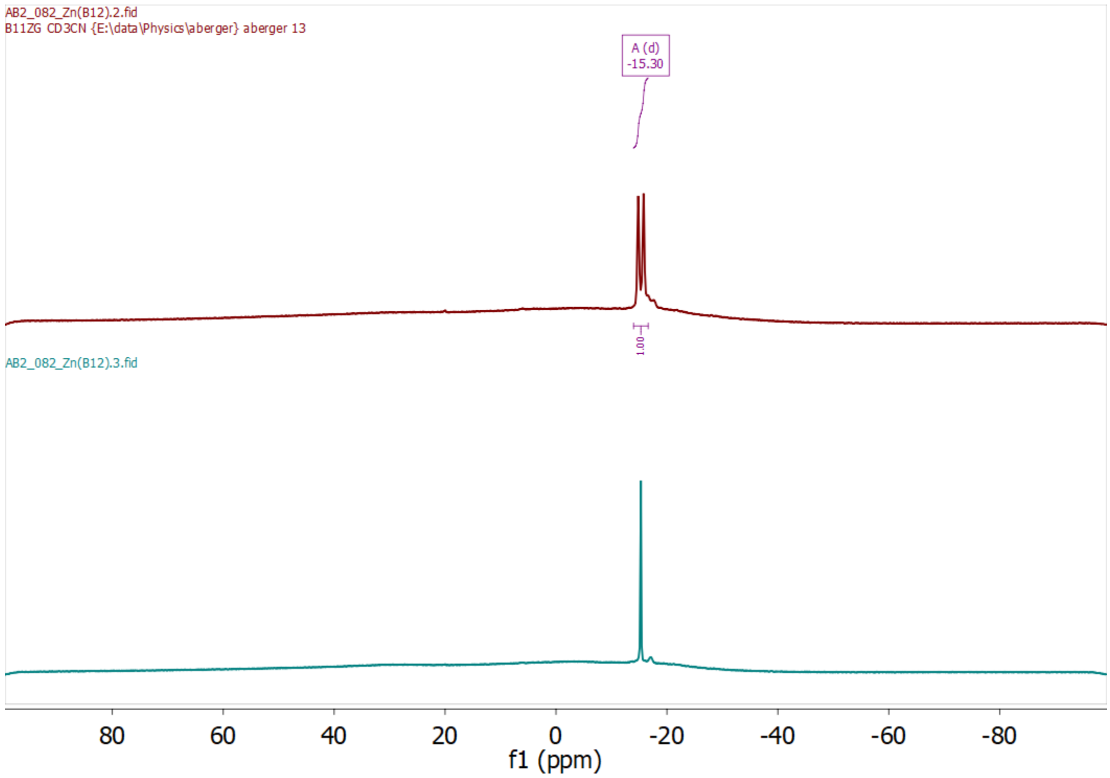

Figure S23: ^{11}B NMR (top) and $^{11}B\{^{1}H\}$ NMR (bottom) for $Zn[B_{12}H_{12}]\cdot xH_2O$.

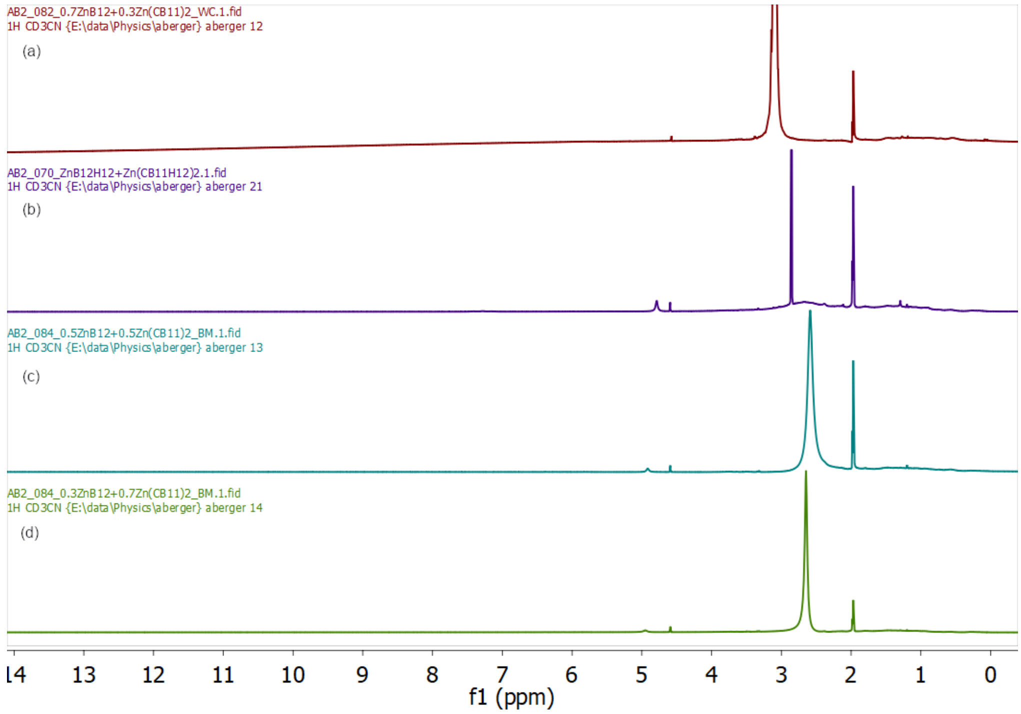

Figure S24: [1]H NMR of (a) $0.7Zn[B_{12}H_{12}]\cdot xH_2O + 0.3Zn[CB_{11}H_{12}]_2\cdot xH_2O$, (b) $0.7Zn[B_{12}H_{12}]\cdot xH_2O + 0.3Zn[CB_{11}H_{12}]_2\cdot xH_2O$ + BM, (c) $0.5Zn[B_{12}H_{12}]\cdot xH_2O + 0.5Zn[CB_{11}H_{12}]_2\cdot xH_2O$ + BM, and (d) $0.3Zn[B_{12}H_{12}]\cdot xH_2O + 0.7Zn[CB_{11}H_{12}]_2\cdot xH_2O$.

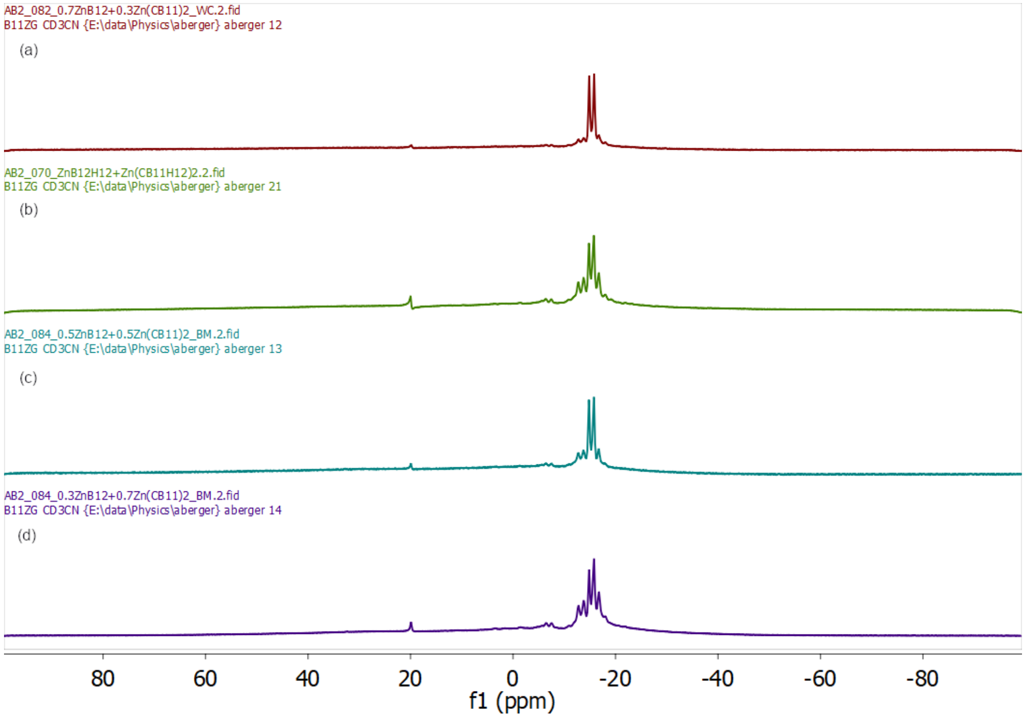

Figure S25: [11]B NMR of (a) $0.7Zn[B_{12}H_{12}] \cdot xH_2O + 0.3Zn[CB_{11}H_{12}]_2 \cdot xH_2O$, (b) $0.7Zn[B_{12}H_{12}] \cdot xH_2O + 0.3Zn[CB_{11}H_{12}]_2 \cdot xH_2O$ + BM, (c) $0.5Zn[B_{12}H_{12}] \cdot xH_2O + 0.5Zn[CB_{11}H_{12}]_2 \cdot xH_2O$ + BM, and (d) $0.3Zn[B_{12}H_{12}] \cdot xH_2O + 0.7Zn[CB_{11}H_{12}]_2 \cdot xH_2O$.

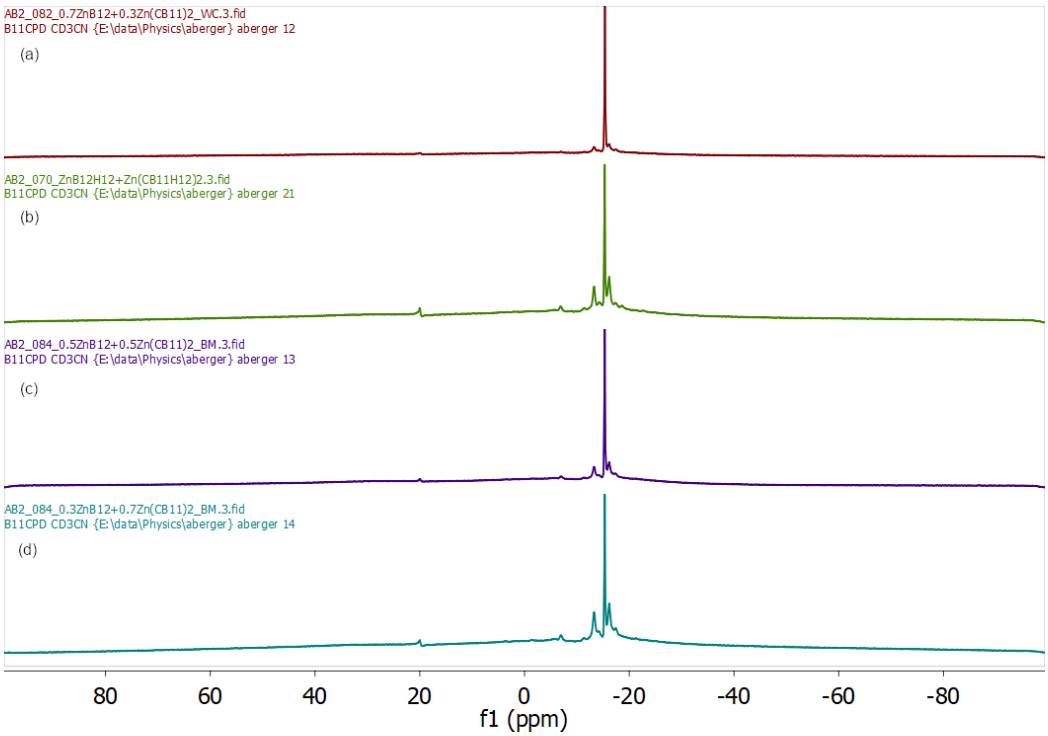

Figure S26: [11]B{[1]H} NMR of (a) $0.7Zn[B_{12}H_{12}] \cdot xH_2O + 0.3Zn[CB_{11}H_{12}]_2 \cdot xH_2O$, (b) $0.7Zn[B_{12}H_{12}] \cdot xH_2O + 0.3Zn[CB_{11}H_{12}]_2 \cdot xH_2O$ + BM, (c) $0.5Zn[B_{12}H_{12}] \cdot xH_2O + 0.5Zn[CB_{11}H_{12}]_2 \cdot xH_2O$ + BM, and (d) $0.3Zn[B_{12}H_{12}] \cdot xH_2O + 0.7Zn[CB_{11}H_{12}]_2 \cdot xH_2O$.

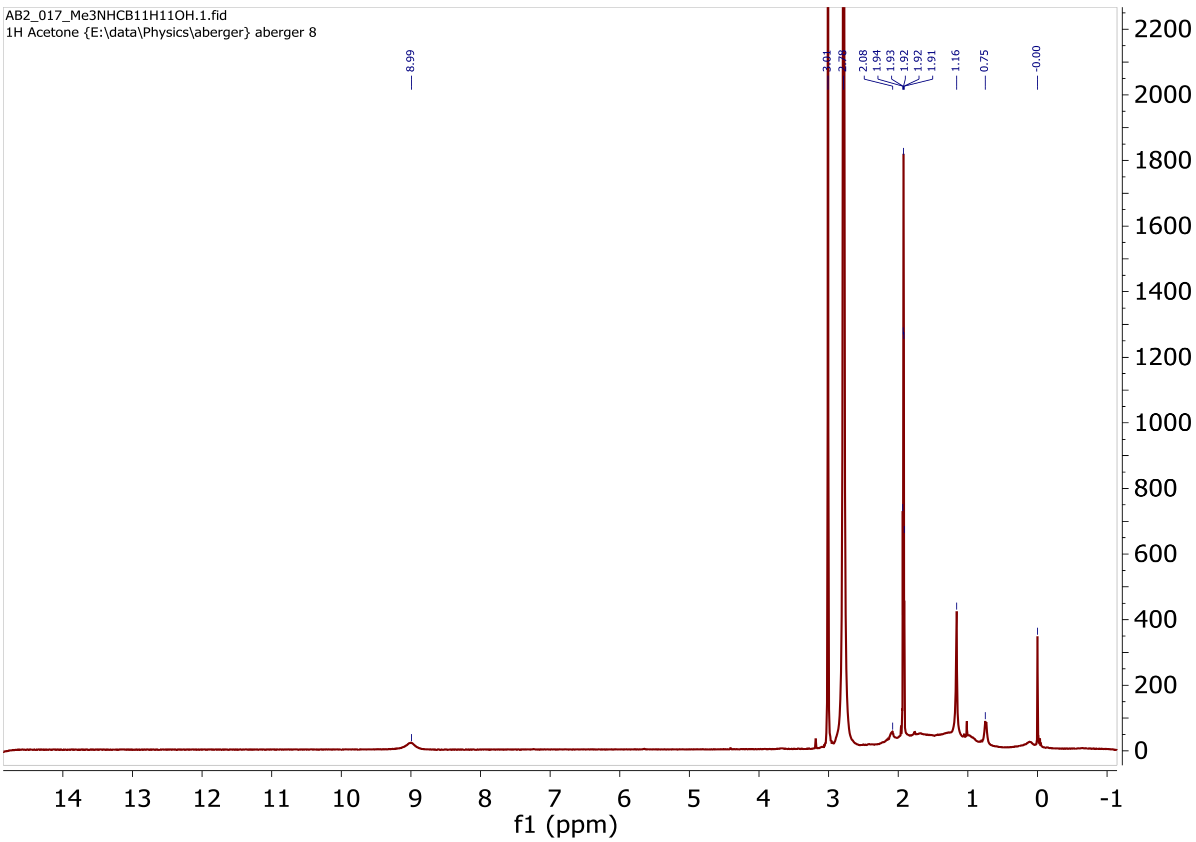

Figure S27: ${}^{1}H$ NMR of $Me_3NH[12\text{-}OH\text{-}CB_{11}H_{11}]$ in acetone-d6

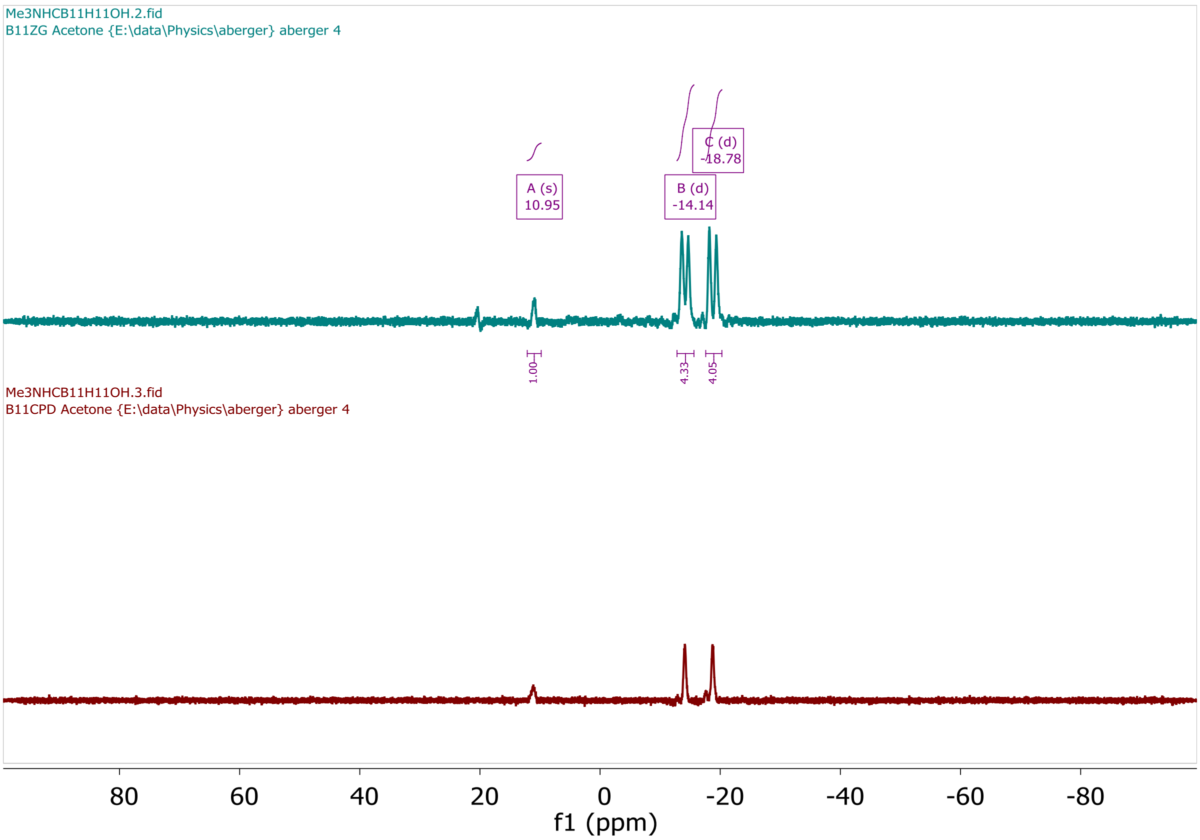

Figure S28: ${}^{11}B$ (top) and ${}^{11}B\{{}^{1}H\}$ (bottom) NMR of $Me_3NH[12\text{-}OH\text{-}CB_{11}H_{11}]$ in acetone-d6.

Nyquist plots.

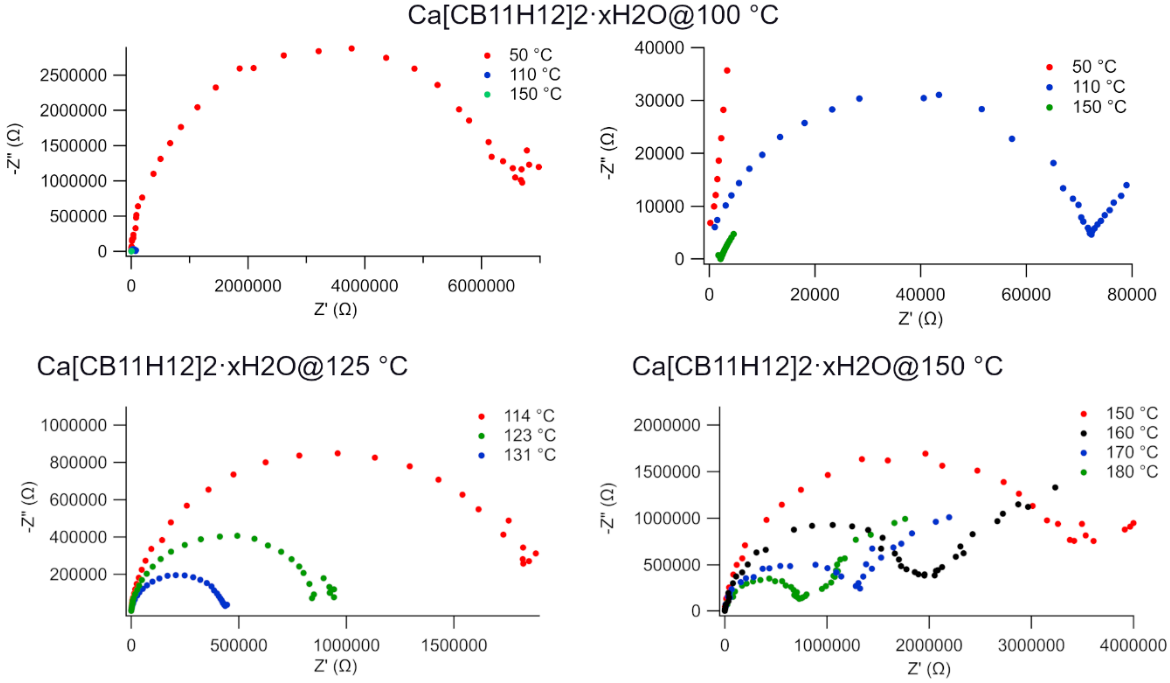

Figure S29: Nyquist plots for Ca[$CB_{11}H_{12}$]$_2$·$x$$H_2O$ dried at 100 °C, 125 °C and 150 °C.

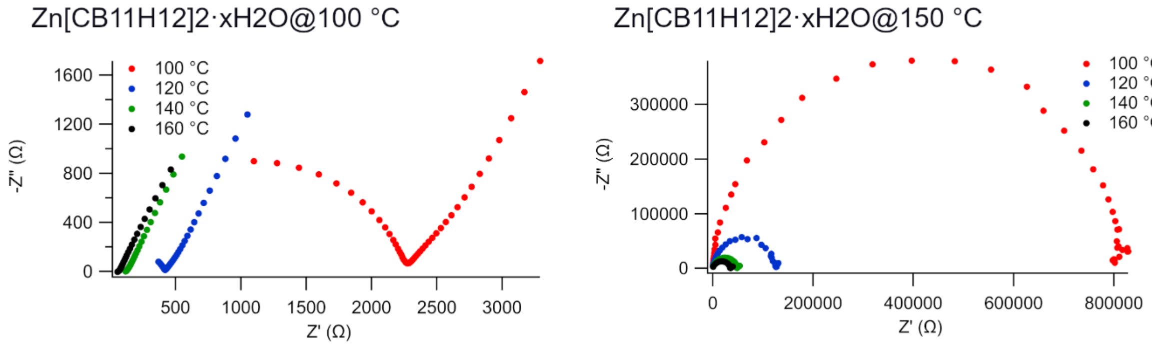

Figure S30: Nyquist plots for Zn[$CB_{11}H_{12}$]$_2$·$x$$H_2O$ dried at 100 °C and 150 °C.

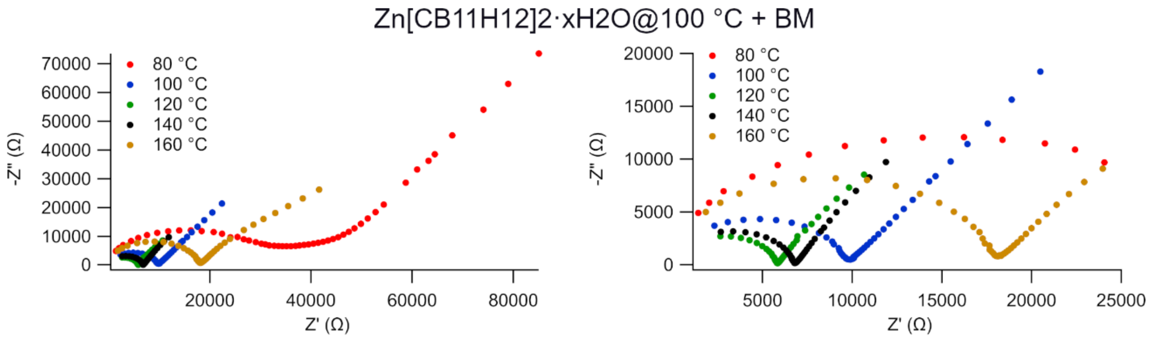

Figure S31: Nyquist plots for $Zn[CB_{11}H_{12}]_2{\cdot}xH_2O$@100 °C + BM (ball milling).

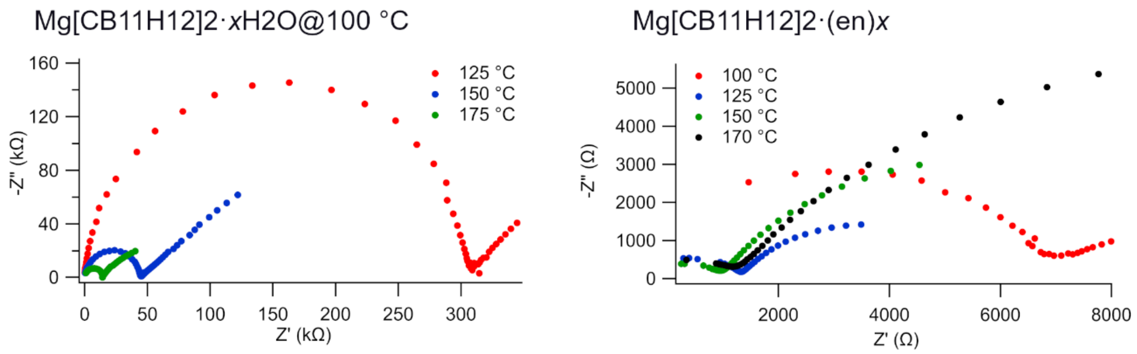

Figure S32: Nyquist plots for $Mg[CB_{11}H_{12}]_2{\cdot}xH_2O$@100 °C and $Mg[CB_{11}H_{12}]_2{\cdot}3en$.

References

1 X. Chen, H. K. Lingam, Z. Huang, T. Yisgedu, J. C. Zhao and S. G. Shore, Thermal decomposition behavior of hydrated magnesium dodecahydrododecaborates, *J. Phys. Chem. Lett.*, 2010, **1**, 201–204.